Sensitivity Analysis of an MPC-based Motion Cueing Algorithm for a Curve Driving Scenario

van der Ploeg, J.R.; Cleij, D.; Pool, D.M.; Mulder, Max; Bülthoff, Heinrich H.

Important note
To cite this publication, please use the final published version (if applicable).
Please check the document version above.

Sensitivity Analysis of an MPC-based Motion Cueing Algorithm for a Curve Driving Scenario

Joost R. van der Ploeg[1,2]**, Diane Cleij**[1,2]**, Daan M. Pool**[1]**, Max Mulder**[1] **and Heinrich H. Bülthoff**[2]

(1) Delft University of Technology, Faculty of Aerospace Engineering, Control & Simulation section, 2629 HS Delft, e-mail : {d.m.pool, m.mulder}@tudelft.nl
(2) Max Planck Institute for Biological Cybernetics, Motion Perception and Simulation Group, 72076 Tübingen, e-mail : {diane.cleij, heinrich.buelthoff}@tuebingen.mpg.de

Abstract - Despite gaining popularity, the use of Motion Cueing Algorithms (MCAs) based on Model Predictive Control (MPC) remains challenging due to the required tuning of a large number of cost function parameters. This paper investigates the effects of two critical MPC cost function parameters, the lateral specific force and roll rate error weights (W_{a_y} and W_p), on the motion cueing quality achieved with an MPC-based MCA for a curve driving scenario. An offline sensitivity analysis, which quantified the effects of varying W_{a_y} and W_p on the Root Mean Square Error (RMSE) and Pearson Correlation Coefficient (PCC) of the resulting simulator motion outputs, shows that for the same percentage-wise variation, W_{a_y} has a more pronounced effect on both cueing quality predictors than W_p. In addition, for both RMSE and PCC, the effects of W_{a_y} and W_p are also found to be largely independent, i.e., without interaction effects. This was further tested in a passive human-in-the-loop experiment with 20 participants and with nine different W_{a_y} and W_p parameter combinations as test conditions, performed in the hexapod moving-base simulator of the Max Planck Institute for Biological Cybernetics in Tübingen. The collected continuous rating data, which were found to be reliable for 18/20 participants, show a statistically significant variation across all experiment conditions, and especially a strong interaction effect of W_{a_y} and W_p. Somewhat surprisingly, the overall lowest continuous ratings were given to the combination of both reference weight settings from earlier research (our baseline condition). In line with the interaction effect in the continuous data, an extended post-experiment correlation analysis shows that a weighted combination of lateral specific force RMSE and and roll rate RMSE above the roll rate perception threshold strongly correlates ($\rho = 0.98$) with the variation in mean continuous ratings across all experiment conditions. This approach can potentially be used for straightforward prediction of perceived motion cueing quality and offline MCA optimization.

Keywords: motion cueing, driving simulators, curve driving, model predictive control, continuous subjective ratings

Introduction

In recent years, Motion Cueing Algorithms (MCAs) based on Model Predictive Control (MPC) have become more popular [Dag09, Bas11, Gar13, Kat15]. The main reason for this is the fact that, unlike classical filter-based MCAs [Gra97], MPC can explicitly account for physical limits of simulators' workspaces and therefore use the available motion space more effectively. Multiple recent comparisons between filter-based MCAs and newly developed MPC-based MCAs indeed confirm that MPC has the potential to enable much-improved motion cueing quality [Cle18, Gar13].

While many different MPC-based MCAs have been proposed [Dag09, Bas11, Gar13, Kat15], the main principle of MPC – its use of a *cost function* to find a "current" optimal control input accounting for the current controlled system state as well as its future trajectory – is common to all implementations. Furthermore, the cost function of an MPC-based MCA typically contains many parameters that need to be tuned to achieve satisfactory motion cueing quality. Especially for online driver-in-the-loop MPC cueing, this parameter tuning is critical, due to the re-

quired use of limited prediction horizons and inaccurate model predictions [Kat15, Beg12], to reduce computational costs. While the parameters (i.e., cost function weights) of an MPC-based MCA can perhaps be considered to be more intuitive to tune than the parameters of a filter-based MCA (e.g., damping ratios and cut-off frequencies), the large number of parameters (e.g., 39 cost function weight parameters [Kat17, Kat18]) and their interactions that together result in an MCP-based MCA output in fact make this a highly complex problem in practice.

The goal of this paper is to investigate the effects of two critical parameters of an MPC-based MCA's cost function on the motion cueing quality for a curve driving scenario: the lateral specific force and roll rate error weights, W_{a_y} and W_p. This paper will present an offline sensitivity analysis performed on the MPC-based MCA developed at the Max Planck Institute (MPI) for Biological Cybernetics [Kat15, Kat17, Kat18], but as equivalent weight parameters are present in all MPC implementations these results will be of general interest. In addition to the sensitivity analysis, this paper presents the results of a human-in-the-loop experiment performed

in the hexapod moving-base simulator of the MPI for Biological Cybernetics, in which 20 participants used continuous ratings to assess different W_{a_y} and W_p settings in a passive curve driving scenario.

MPC motion cueing

In an MPC-based MCA, an explicit optimisation of the future trajectory of the simulator is performed using a cost function that minimises the squared error between reference values and actual values of the selected output variables ($\mathbf{y}_k$), state variables ($\mathbf{x}_k$), input variables ($\mathbf{u}_k$) and the terminal state ($\mathbf{x}_N$), over a prediction horizon of N future samples [Kat17]. Such a cost function is given in (1):

$$
\begin{aligned}
\mathbf{u}_k = \arg\min_{\mathbf{u}_k} \frac{1}{N} \sum_{k=1}^{N} \Big[& W_y \left(\mathbf{y}(\mathbf{x}_k, \mathbf{u}_k) - \hat{\mathbf{y}}_k \right)^2 \\
& + W_x \left(\mathbf{x}_k - \hat{\mathbf{x}}_k \right)^2 + W_u \left(\mathbf{u}_k - \hat{\mathbf{u}}_k \right)^2 \Big] \\
& + W_{x_N} ||\mathbf{x}_N - \hat{\mathbf{x}}_N||^2
\end{aligned} \quad (1)
$$

In MPC-based MCAs, the output term of (1) is generally used to penalize differences between simulator $\mathbf{y}(\mathbf{x}_k, \mathbf{u}_k)$ and real vehicle $\hat{\mathbf{y}}_k$ motion outputs, while the state term $\mathbf{x}_k - \hat{\mathbf{x}}_k$ provides "washout" by limiting the simulator attitude and position $\mathbf{x}_k$ compared to its neutral position $\hat{\mathbf{x}}_k$. Furthermore, the input term $\mathbf{u}_k - \hat{\mathbf{u}}_k$ provides input limiting, while the terminal state error term provides an explicit means to ensure that the simulator state remains bounded, to improve algorithm stability. The key to effective application of an MPC cost function as given by (1) is its *tuning*, i.e., selecting appropriate values for the parameters that influence the trade-off made by the MPC algorithm. In (1) these tunable parameters are indicated as the weighting matrices W_y, W_u, W_x and W_{x_N}, which are generally all diagonal matrices with error weight parameters on their diagonals, which can be increased for a higher penalty on the corresponding squared error term in solving for the optimal $\mathbf{u}_k$.

For the MPC-based MCA considered in this paper [Kat17], the MPC output vector $\mathbf{y}$, state vector $\mathbf{x}$, and input vector $\mathbf{u}$ are defined in (2) to (4). The output vector $\mathbf{y}$ consists of motion states the human vestibular system is sensitive to: the specific forces (a_x, a_y, a_z), rotational rates (p, q, r), and rotational accelerations ($\dot{p}$, $\dot{q}$, $\dot{r}$). The state vector $\mathbf{x}$ contains the simulator cabin position (x, y, z) and attitude (ϕ, θ, ψ), as well as their time derivatives. The input vector $\mathbf{u}$ contains the outputs of the MCA, i.e., the setpoints for the motion control system of the simulator platform, here expressed as specific forces (a_x, a_y, a_z) and rotational accelerations ($\dot{p}$, $\dot{q}$, $\dot{r}$) in simulator body axes. With this definition of the output, input, and state vectors, the MPC cost function of (1) requires a total of 39 weight parameters (W_y, W_x, W_u W_{x_N}) and an equal number of reference values ($\hat{\mathbf{y}}_k$, $\hat{\mathbf{x}}_k$, $\hat{\mathbf{u}}_k$, $\hat{\mathbf{x}}_N$) to be tuned, for which the baseline values used in this paper are listed in Table 1

$$
\mathbf{y} = \begin{bmatrix} a_x & a_y & a_z & p & q & r & \dot{p} & \dot{q} & \dot{r} \end{bmatrix}^T \quad (2)
$$

$$
\mathbf{x} = \begin{bmatrix} x & y & z & \phi & \theta & \psi & \dot{x} & \dot{y} & \dot{z} & p & q & r \end{bmatrix}^T \quad (3)
$$

$$
\mathbf{u} = \begin{bmatrix} a_x & a_y & a_z & \dot{p} & \dot{q} & \dot{r} \end{bmatrix}^T \quad (4)
$$

As can be verified from Table 1, for W_y the weights on rotational acceleration errors were set to 0, while the specific force and rotational velocity error weights were chosen to roughly compensate for the average magnitude difference of specific forces (in m/s²) and angular velocities (in rad/s) during typical vehicle manoeuvres [Kat17]. Both the input error weights (W_u) and terminal state weights (W_{x_N}) were set to very small values (0.01), to effectively omit input limiting and the stabilizing effect of a terminal state penalty, as in general there is no need for both on a hexapod-based motion simulator. Finally, the state error weights W_x listed in Table 1 were obtained from an optimization for the current curve driving scenario, to ensure that the simulator platform would move back to its neutral position and attitude within a reasonable time span after a curve. This tuning of W_x was essential to ensure that the motion platform was again in its neutral position before a next curve would start in our simulated curve driving scenario.

In addition to the weight factors, an MPC cost function requires reference trajectories for all outputs, states, and inputs against which errors should be minimised, i.e., $\hat{\mathbf{y}}_k$, $\hat{\mathbf{x}}_k$, $\hat{\mathbf{u}}_k$, and $\hat{\mathbf{x}}_N$ in (1), see also Table 1. First, the state reference $\hat{\mathbf{x}}_k$ represents the state towards which the motion platform will perform washout, i.e., generally the motion platform's neutral position. In addition, to achieve their respective intentions, the input ($\hat{\mathbf{u}}_k$) and terminal state ($\hat{\mathbf{x}}_N$) references are generally also set to zero. Finally, for most MPC problems defining and calculating the output reference $\hat{\mathbf{y}}_k$, i.e., a prediction of the reference output along the prediction horizon, is the key aspect of MPC controller design, where most differences in implementation are observed. While for passive simulations the (known) true future vehicle trajectory could be used for $\hat{\mathbf{y}}_k$, here we choose to explicitly focus on an implementation that can also be implemented in real time: a "constant" prediction strategy, for which it is assumed that there will be no change in the vehicle motion during the prediction horizon. For MPC-based MCAs that need to run in real-time, currently the prediction horizon is generally limited by available computational power. Here, a real-time feasible prediction horizon of 2 s with a time step of Δt = 0.1 s and hence N = 20 prediction steps is used.

Methodology
Scenario and Test Conditions

To tie in with earlier experiments [Cle18, Lee19], in this paper we focus on motion cueing for a curve driving scenario. The reference vehicle motion for the driven curves was generated in CarSim [Car17] and was tuned to result in a "nominal" trajectory with a maximum sustained lateral specific force of approximately 2 m/s² during the sustained part of the curve.

In addition, in this paper we focus on the combination of an offline sensitivity analysis and a human-in-the-loop simulator experiment to study the effects of the two MPC cost function weight parameters that most directly affect the cueing quality in curve driving: the lateral specific force error weight W_{a_y} and the roll rate error weight W_p, two elements in W_y as defined in (1). As can be verified from Table 2, with respect to the baseline weights of W_{a_y}=1 and W_p=10 [Kat15] (our condition C5, indicated in bold in Table 2), for

Table 1. Overview of the parameter values of the cost function of the MPC-controller in the baseline configuration.

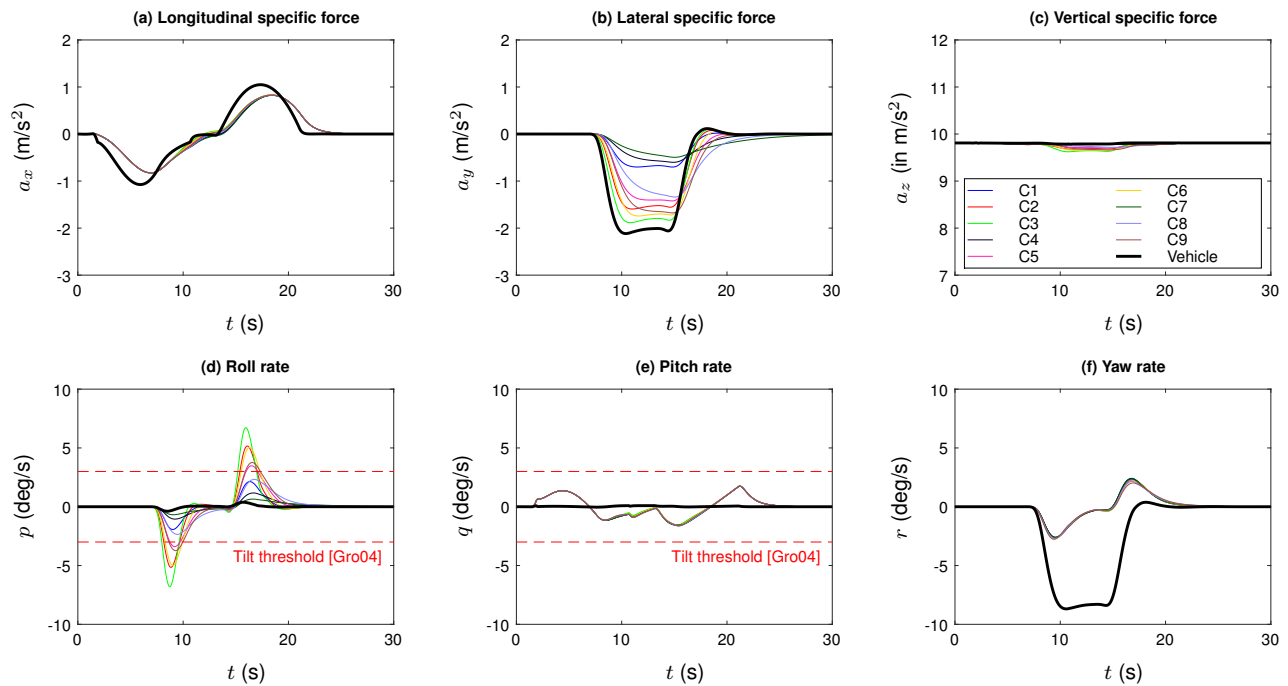|	Parameter	Spec. forces $a_x\ a_y\ a_z$	Rot. vel. $p\ q\ r$	Rot. accel. $\dot{p}\ \dot{q}\ \dot{r}$
Outputs and *Inputs*	W_y	1 1 1	10 10 10	0 0 0
	$\hat{y}_k$	"Constant" prediction ($N = 20$ and $\Delta t = 0.1$ s)		
	W_u	0.01 0.01 0.01	–	0.01 0.01 0.01
	$\hat{u}_k$	0 0 0	–	0 0 0
	Parameter	Position $x\ y\ z$	Attitude $\phi\ \theta\ \psi$	Lin. vel. $\dot{x}\ \dot{y}\ \dot{z}$	Rot. vel. $p\ q\ r$
States and *Terminal States*	W_x	8.2 5.1 3.6	5.4 3.7 6.8	0 0 0	0 0 0
	$\hat{x}_k$	0 0 0	0 0 0	0 0 0	0 0 0
	W_{x_N}	0.01 0.01 0.01	0.01 0.01 0.01	0.01 0.01 0.01	0.01 0.01 0.01
	$\hat{x}_N$	0 0 0	0 0 0	0 0 0	0 0 0

Figure 1. The output of the simulator for all nine experiment conditions, including perception thresholds for tilt rates.

both weights additional values that were 60% higher and lower were tested. Both parameters were varied independently, meaning that in total the full factorial of nine conditions is investigated.

Table 2. Test conditions with different W_{a_y} and W_p weights.

		W_{a_y}		
		0.4	1.0	1.6
W_p	4	C1	C2	C3
	10	C4	**C5**	C6
	16	C7	C8	C9

Fig. 1 shows the time traces of the simulator outputs for all nine test conditions. The vehicle motion (Car-Sim data) is shown with a thick black line for reference. Also indicated in the Fig. 1(d) and (e) with red dashed lines is the perception threshold for tilt rates of 3 deg/s [Gro04] (0.0524 rad/s). This simulator roll rate results from tilt commanded by the MPC cueing to better match the sustained lateral acceleration (a_y)

during the curves. Fig. 1 shows that for conditions with low W_p and high W_{a_y} – e.g., C2, C3, and C6 – the simulator roll rate responses exceed the perception threshold.

Offline sensitivity analysis

In the offline sensitivity analysis, both the individual effects of varying only W_{a_y} or W_p over a wide range of values, as well as interaction effects due to concurrent variations in both weight parameters, were investigated explicitly. In this paper, however, only the results for the set of parameter combinations of Table 2 are presented for brevity. To be able to quantify both magnitude and phase (shape) cueing errors [Gra97, CY15, Ber13], two objective metrics were considered as predictors of motion cueing quality in the sensitivity analysis: the Root Mean Square Error (RMSE, see (5)), which penalizes both magnitude and shape errors, and the Pearson Correlation Coefficient (PCC, see (6)), which penalises shape errors.

$$\text{RMSE}(a_y) = \sqrt{\frac{1}{N}\sum_{k=1}^{N}(a_{y_k} - \hat{a}_{y_k})^2} \qquad (5)$$

$$\text{PCC}(a_y) = \frac{1}{N-1}\sum_{k=1}^{N}\left(\frac{a_{y_k} - \mu_{a_y}}{\sigma_{a_y}}\right)\left(\frac{\hat{a}_{y_k} - \mu_{\hat{a}_y}}{\sigma_{\hat{a}_y}}\right) \qquad (6)$$

In (5) and (6), N is number of data points, a_y and $\hat{a}_y$ represent the simulator and vehicle (reference) lateral specific forces, and μ and σ indicate mean and standard deviation, respectively. Note that while (5) and (6) show how both metrics are calculated for the lateral specific force a_y, the same equations can be used for all other simulator outputs as well.

As a reference for the RMSE and PCC values calculated for an MPC-based MCA in our sensitivity analysis, the same two metrics were also calculated for a representative filter-based Classical Washout Filter (CWF) implementation for curve driving, as reported in [Ven15].

Simulator experiment

Experiment participants and procedures

In the experiment, 20 participants were subjected to the same passive curve driving scenario (i.e., they were passengers) under the nine different MCA settings of Table 2 and Fig. 1. In each experiment trial, all nine test conditions were presented back to back, i.e., a single trial consisted of nine randomized curves, each with a different W_{a_y} and W_p combination. In these trials, an initial acceleration and final deceleration were included for a more realistic simulation scenario.

Throughout each trial, participants provided Continuous Ratings (CRs) of their perceived motion incongruence according to the procedure outlined in [Cle18] as the main outcome variable that was compared to the sensitivity analysis results. With this CR, participants were asked to continuously indicate to what extent they felt a mismatch between the vehicle motion that was presented visually and through the platform motion, i.e., their perceived motion incongruence as a function of time during the simulation. As part of the continuous rating method [Cle18], two training trials were performed before collecting the measurements, to allow participants to familiarize themselves with the method and the platform cueing for the different test conditions. After the training trials, participants performed three repeated measurement trials, to be able to quantify whether participants rated consistently. One simulator trial lasted approximately 6 minutes.

Finally, to help in the interpretation of the CR results, participants were asked to fill in a questionnaire after the experiment, in which participants were asked structured questions to find out how they decided on a certain rating (not presented here, see [Plo18]). Also, after each trial participants were asked to provide a sickness score (MISC) [Bos05], to monitor motion sickness development during the experiment. Overall, however, motion sickness was not an issue in this experiment.

Apparatus

The experiment was performed in the hexapod moving-base simulator of the MPI for Biological Cybernetics in Tübingen, see Fig. 2(a), which has a Bosch Rexroth eMotion-1500-6DOF-650-MK1 motion platform. During the experiment, participants were presented with computer-generated visuals (generated with Unity) projected on a screen in front of them, see Fig. 2(b), that matched the true (CarSim) vehicle motion (i.e., the thick black lines in Fig. 1). Participants provided their CRs by turning a knob mounted in front of them on the simulator platform, see Fig. 2(c). In addition, as also shown in Fig. 2(c), a "rating bar" was shown on the screen to provide participants with continuous visual feedback of their own current rating.

Data Analysis

The only dependent variable measured in the experiment was the CR, for which three repeated measurements were collected from each participant. Before further analysis of the CR data, the consistency of participants' rating data was verified using Cronbach's alpha [Cro51], a measure of internal consistency. Table 3 shows the Cronbach's alpha values for all 20 participants. Table 3 shows that the CRs provided by two participants (10 and 18) shows poor consistency (Cronbach's alpha < 0.7). Hence, the data provided by these two participants were excluded from further analysis.

Table 3. Cronbach's alpha values for all participants. Bold values indicate inconsistent participants.

Subj. #	Cronbach's alpha	Subj. #	Cronbach's alpha
1	0.8848	11	0.9174
2	0.9536	12	0.9059
3	0.8604	13	0.9273
4	0.9325	14	0.9224
5	0.9106	15	0.9609
6	0.9151	16	0.8225
7	0.9219	17	0.8487
8	0.8945	**18**	**0.6180**
9	0.9181	19	0.8650
10	**0.2326**	20	0.9715

The raw CR data for the consistent participants were averaged across the three repeated trials to calculate an "average" CR time trace that was used for further analysis. The main metric used to compare the CRs across the nine test conditions was the mean CR, in this paper indicated as $\overline{CR}$, calculated as the time-average rating across each 30-second curve segment. The variation in the mean CR was explicitly compared between conditions using statistical analysis (repeated-measures ANOVA).

Finally, to link the results from the sensitivity analysis (RMSE and PCC) and the experiment (CR), an explicit correlation analysis was performed (using Pearson's correlation coefficient ρ) between the measured $\overline{CR}$ data and predictions of these CRs (i.e., $\widehat{CR}$) based on the RMSE and PCC for a_y or p or a weighted combination of both.

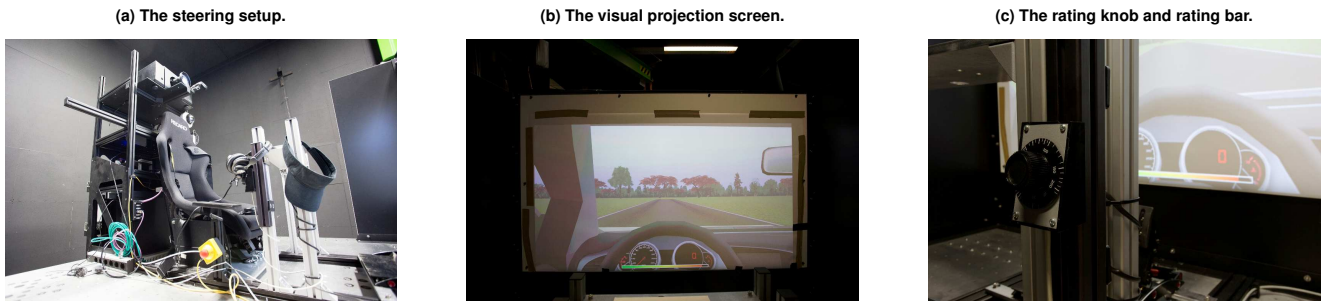|		
(a) The steering setup.	**(b) The visual projection screen.**	**(c) The rating knob and rating bar.**

Figure 2. The experiment setup in the MPI hexapod simulator, showing the steering setup (a), the visuals and projection screen (b), and the turning knob participants used to provide their continuous rating (c). In (c) the rating bar on the screen also shows the current rating.

Results and discussion

Sensitivity analysis

Figures 3 and 4 show the RMSE and PCC values for all experiment conditions for the considered curve driving scenario, respectively. In all figures, the different W_{a_y} settings are on the x-axis, while the different settings for W_p (4, 10, and 16) are presented with blue, red, and yellow markers, respectively. In addition, with a solid gray line all figures present the RMSE or PCC values for the reference Classical Washout Filter (CWF) from [Ven15]. Finally, note that for visual consistency with the RMSE data of Fig. 3, Fig. 4 presents the PCC data with an inverted y-axis, as a high PCC indicates better cueing.

As expected, W_{a_y} directly influences the tracking performance for the lateral specific force (see Fig. 3(b)), i.e., increasing W_{a_y} reduces RMSE(a_y), at the cost of more perceptible false cues in roll rate due to stronger tilt coordination. Though a less strong effect for the same percentage-wise variation in cost function weight, W_p is found to have the opposite effects on both RMSE(a_y) and RMSE(p), i.e., reduced roll rate errors with high W_p, at the cost of increased RMSE(a_y). Finally, as can be verified from Fig. 3, the RMSE for all other degrees-of-freedom (a_x, a_z, q, r) only shows negligible effects of both W_{a_y} and W_p.

For the PCC, Fig. 4(b) shows a variation with W_{a_y} and W_p that is mostly consistent with the RMSE data in Fig. 3(b). Increasing W_{a_y} and decreasing W_p are found to result in a PCC(a_y) that is closer to unity and hence better cueing (reduced shape errors). Somewhat counter-intuitively, Fig. 4(d) shows that increasing W_p results in reduced PCC(p), indicative of increased shape errors in roll cueing. This can be explained by considering the time responses for p shown in Fig. 1(d), where the phase lag in the roll rate peaks compared to the (low magnitude) vehicle roll rates is seen to be reduced for the bigger peaks that occur with high W_{a_y} and/or low W_p. Finally, while PCC(a_x), PCC(q), and PCC(r) show hardly any effect of both W_{a_y} and W_p (just as was found for the RMSE), the PCC for the vertical specific force a_z is seen to show an even larger variation with both weights than seen for both a_y and p. Considering Fig. 1(c) this can be attributed to, in terms of absolute value, very small differences in a_z cueing as a result of the roll tilt. Overall, the fact that the PCC is

only sensitive to shape errors, while the magnitude of cueing errors are not taken into account, thus degrades the usefulness of the PCC as a predictor of motion cueing quality for the curve driving scenario considered in this paper.

From the sensitivity analysis it was thus found that both W_{a_y} and W_p have a significant impact on MPC-based MCA cueing quality for the key degrees-of-freedom in a curve driving scenario, i.e., a_y and p. Increasing W_{a_y} results in the expected improved replication of vehicle lateral specific forces, both in terms of RMSE and PCC, at the cost of increased roll tilt. Increasing the roll rate error weight W_p will suppress roll tilt, which only affects simulator roll during the curve onsets and exits (see Fig. 1) where tilt coordination is active. Overall, Figures 3 and 4 show that the effects of W_{a_y} and W_p are mostly independent and additive, as for the tested range of parameter settings no dominant interaction effects were observed. Finally, the CWF data presented in Figures 3 and 4 also highlight that with appropriate choice of cost function weights, substantial improvements in RMSE or PCC can be achieved with an MPC-based MCA.

Simulator experiment

Fig. 5 shows the mean CR over time, averaged across all participants, for all experiment conditions and the entire driven curve segment. Please note that for easy comparison, the same colors are used for the different experiment conditions as in Fig. 1. Fig. 5 clearly shows, as was also found in earlier experiments [Lee19], that participants on average reported the largest perceived incongruence (highest CR) during the sustained part of the curve. Furthermore, the highest CRs are consistently given to the conditions with the low W_{a_y} = 0.4 setting (C1, C4, C7), while our baseline condition (C5) is rated best (lowest CR) by the experiment participants. During the curve onset and exit, condition C3 – with the highest W_{a_y} and lowest W_p and thus the highest tilt roll rates, see Fig. 1 – is clearly awarded the highest CRs. Consistent with the sensitivity analysis data of Figures 3 and 4, the CR data in Fig. 5 also show that, for the same percentage-wise variation, W_{a_y} causes a larger change in the provided CRs than W_p.

Fig. 6 shows the time-averaged mean rating $\overline{CR}$ per condition, in the same figure format as used for Fig. 3 and 4. The errorbars indicate the 95% confidence
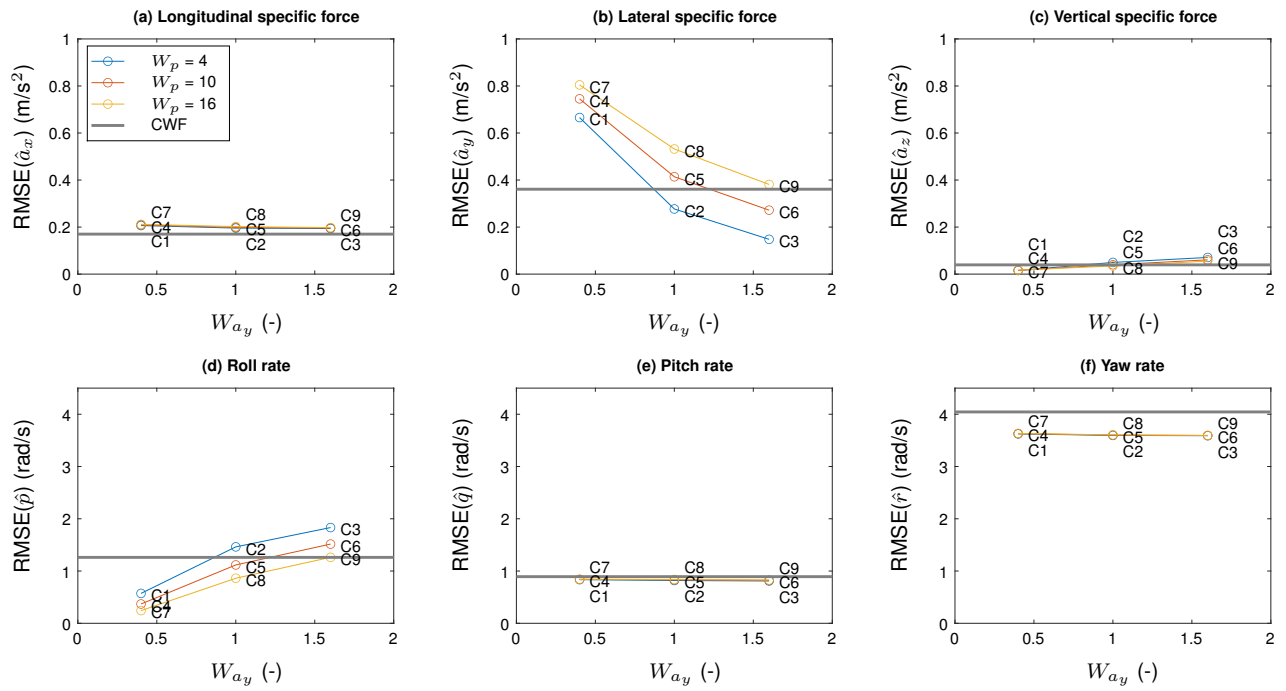
Figure 3. RMSE values for all experiment conditions. The reference Classical Washout Filter (CWF) [Ven15] has been included in gray for comparison.
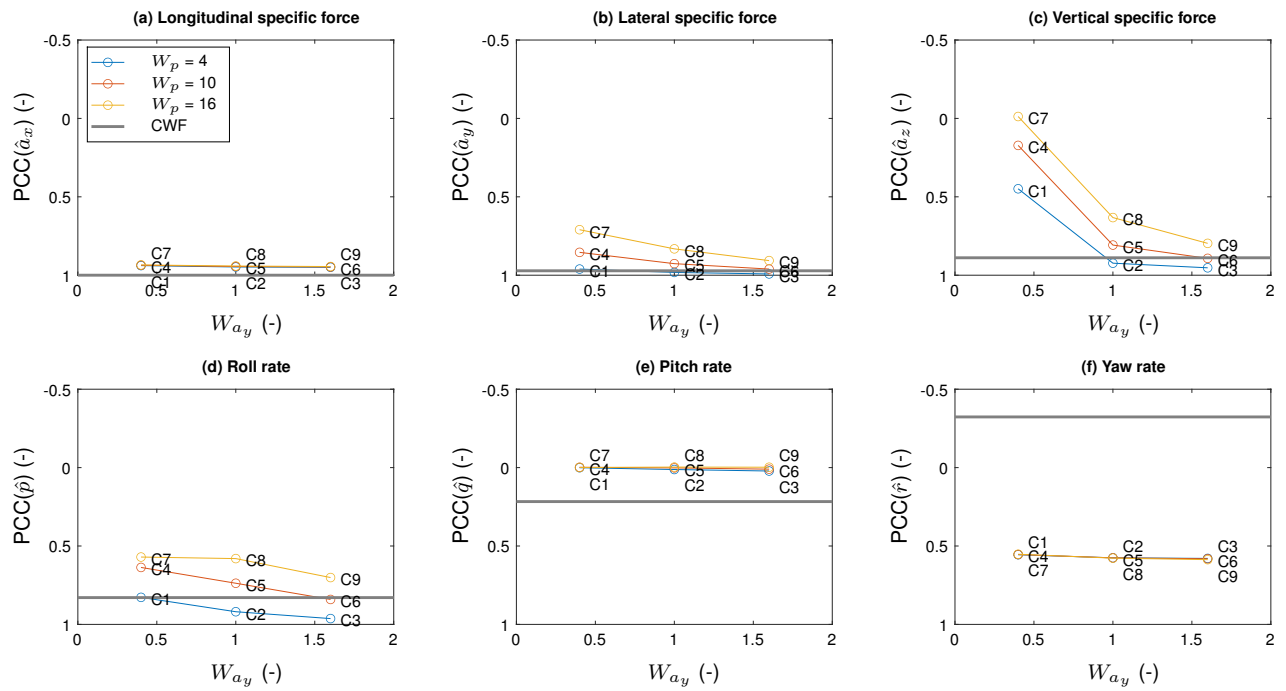

Figure 4. PCC values for all experiment conditions. The reference CWF [Ven15] has been included in gray for comparison.
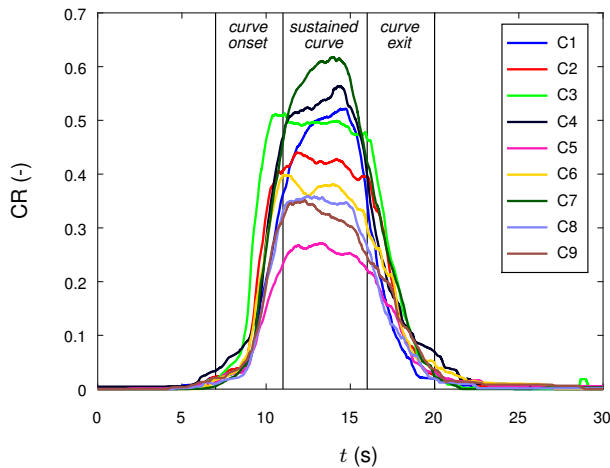
Figure 5. The mean continuous rating (CR) over time for all tested experiment conditions.
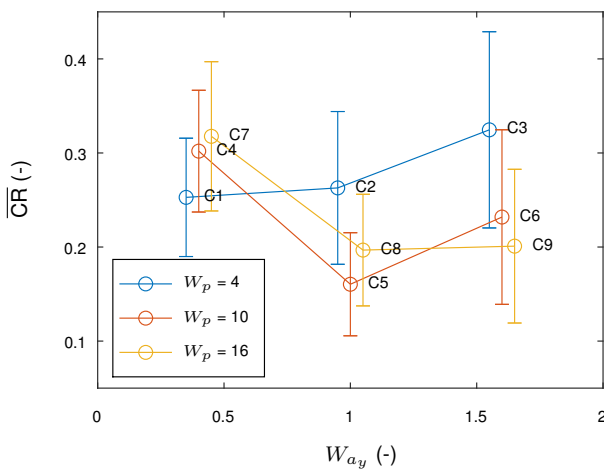

Figure 6. The time-averaged mean rating of across all experiment conditions.

Figure 7. Correlation between the time-averaged mean ratings $\overline{CR}$ and different RMSE predictors $\widehat{CR}$.

how participants' average ratings $\overline{CR}$ might be based on cueing errors in a_y and p, a correlation analysis was performed (by calculating Pearson's correlation coefficient ρ) between the measured time-averaged mean ratings shown in Fig. 6 and the variation in this rating across conditions that would be predicted ($\widehat{CR}$) by the RMSE and PCC, see Figs. 3 and 4. The analysis here is limited the RMSE and PCC for a_y and p, as the sensitivity analysis showed that these are the critical degrees-of-freedom for the considered curve driving scenario. To also account for possible interaction effects, both the individual (a_y or p) correlations between the RMSE/PCC and the mean CR data were calculated, as well as a predictor that used a weighted average of RMSE/PCC in a_y and p.

For the PCC, as perhaps expected based on the sensitivity analysis and Fig. 4, no strong correlations were observed with the CR data: the highest $\rho = 0.18$ was obtained for PCC(a_y). Fig. 7 shows the results for the different considered predictors – RMSE(a_y), RMSE(p), and RMSE(a_y) + $K_p \times$ RMSE(p) – in green dashed, purple dashed, and solid red lines, respectively. As can ben seen in Fig. 7 also the individual RMSE(a_y) and RMSE(p) predictors only result in weak correlations ($\rho < 0.2$). The weighted combination of both RMSE values, however, is found result in a much stronger correlation ($\rho = 0.6$) for a K_p value of around 23 m/s²/(rad/s).

This result can be further improved by comparing the mean rating per experiment condition in Fig. 6 with the RMSE(a_y) data in Fig. 3(b). For most conditions, both figures shows a similar trend, except for conditions C2, C3 and C6, which all resulted in tilt roll rates that far exceeded the perception threshold of 3 deg/s [Gro04]. This suggests that a good indicator of perceived motion quality during curve driving should include RMSE(a_y), but also errors in p above the perception threshold. For this reason, also the RMSE of the roll rate signal from which all values below the perception threshold, indicated as p_{thr}, was considered as a predictor variable. In Fig. 7, the correlation of RMSE(p_{thr}) as well as the combination of RMSE(a_y) and RMSE(p_{thr}) are indicated with a dashed yellow and a solid blue line, respectively.

intervals of the mean $\overline{CR}$ indicated with the circular markers. Fig. 6 again shows that the lowest ratings were given to our baseline condition (C5) with $W_{a_y} = 1$ and $W_p = 10$. Reducing W_{a_y} is seen to, on average, result in increased $\overline{CR}$, while only for high W_{a_y} (1.6), increasing W_p is found to result a better mean rating. A two-way repeated-measures ANalysis Of VARiance (ANOVA) test performed on the mean CR data of Fig. 6 shows a marginally significant direct effect of W_{a_y} ($F(1.2,21.0) = 3.65$, $p = 0.062$) and no significant variation across all conditions due to W_p ($F(1.2,19.7) = 1.69$, $p = 0.211$). Consistent with the observed effects of both cost function weights, a significant interaction effect ($F(2.7,45.1) = 8.08$, $p < 0.001$) is found. Thus, a statistically significant variation in the mean CR across all conditions was measured.

Correlation analysis

Fig. 6 suggests that the MPC-based MCA's weight setting that was rated to be best by participants in the experiment was a compromise between replicating the vehicle lateral acceleration (high W_{a_y}) and limiting false roll tilt rates (high W_p). To further investigate
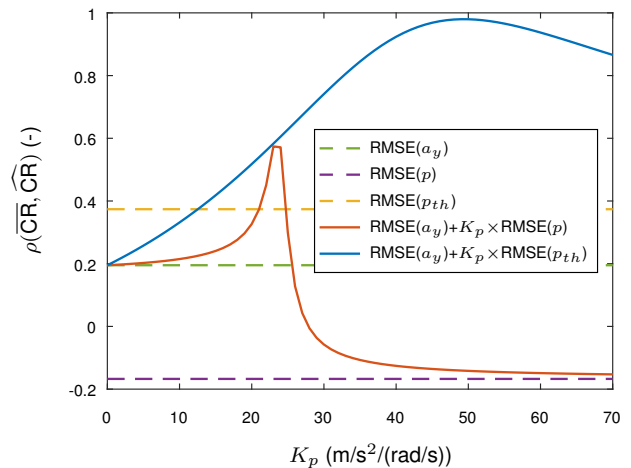
Of all single-variable predictors, the correlation of RMSE(p_{thr}) is found to be highest (0.37). In addition, the combined predictor is found to achieve very high correlation coefficients. For a roll rate weight of 49.4 m/s^2/(rad/s), a maximum correlation of 0.98 is found. This result confirms that perceived motion incongruence for a curve driving scenario, as considered here, can be accurately predicted from a weighted average of RMSE in a_y and p, if small roll rate errors (below threshold) are excluded.

Conclusions/implications

In this paper, the effects of a percentage-wise variation of two key error weight parameters (lateral specific force and roll rate) of the cost function of an MPC-based MCA were investigated for a realistic curve driving scenario. This was done with the combination of an offline sensitivity analysis and a human-in-the-loop driver experiment. The sensitivity analysis, which quantified the effects of varying the lateral specific force (W_{a_y}) and roll rate weight (W_p) parameters using the Root Mean Square Error (RMSE) and Pearson Correlation Coefficient (PCC) as metrics, clearly indicated that with appropriate weight settings better motion cueing than obtained with a reference Classical Washout Filter was achieved with the MPC-based MCA. In addition, the PCC was found to be a less valuable predictor for motion cueing quality, due to the fact that this metric is only sensitive to shape errors (not error magnitude). In the experiment, 18/20 participants provided consistent continuous rating data which also show a statistically significant variation across the tested experiment conditions. Somewhat surprisingly, participants reported the overall lowest continuous perceived mismatch ratings during the curve sections for condition C5 (our baseline condition). In an extended post-experiment correlation analysis, a weighted combination of lateral specific force RMSE and roll error RMSE above the roll rate perception threshold was found to strongly correlate with the variation in mean continuous ratings across all experiment conditions. As this metric explained our experiments' participants' ratings for the different W_{a_y} and W_p settings at very high accuracy ($C = 0.98$), it is potentially a very useful indicator for offline prediction of perceived motion cueing quality and MCA optimization.

References

M. Baseggio, A. Beghi, M. Bruschetta, F. Maran and D. Minen, **An MPC approach to the design of motion cueing algorithms for driving simulators**, in Proceedings of the 2011 14th International IEEE Conference on Intelligent Transportation Systems, Washington, DC, USA, 2011.

A. Beghi, M. Bruschetta and F. Maran, **A real time implementation of MPC based Motion Cueing strategy for driving simulators**, in Proceedings of the 51st IEEE Conference on Decision and Control, Maui, Hawaii, 2012.

A. Berthoz, W. Bles, H. H. Bülthoff, B. J. Correia Grácio, P. Feenstra, N. Filliard, R. Hähne, A. Kemeny, M. Mayrhofer, M. Mulder, H.-G. Nusseck, P. Pretto, G. Reymond, R. Schlässelberger, J. Schwandter, H. J. Teufel, B. Vailleau, M. M. van Paassen, M. Vidal and M. Wentink, **Motion Scaling for High-Performance Driving Simulators**, *IEEE Transactions on Human-Machine Systems*, vol. 43(3): 265–276, 2013.

J. E. Bos, S. N. MacKinnon and A. Patterson, **Motion sickness symptoms in a ship motion simulator: Effects of inside, outside, and no view**, *Aviation, Space, and Environmental Medicine*, vol. 76(12): 1111–1118, 2005.

CarSim, Mechanical Simulation, Ann Arbor (MI), United States, 2017, https://www.carsim.com/products/carsim/index.php.

D. Cleij, J. Venrooij, P. Pretto, D. M. Pool, M. Mulder and H. H. Bülthoff, **Continuous rating of perceived visual-inertial motion incoherence during driving simulation**, in Proceedings of the Driving Simulation Conference 2015 Europe, Tübingen, Germany, 2015.

D. Cleij, J. Venrooij, P. Pretto, D. M. Pool, M. Mulder and H. H. Bülthoff, **Continuous Subjective Rating of Perceived Motion Incongruence During Driving Simulation**, *IEEE Transactions on Human-Machine Systems*, vol. 48(1): 17–29, 2018.

L. J. Cronbach, **Coefficient alpha and the internal structure of tests**, *Psychometrika*, vol. 16(3): 297–334, 1951.

S. Casas-Yrurzurm, I. Coma, J. V. Riera and M. Fernández, **Motion-Cuing Algorithms: Characterization of Users' Perception**, *Human Factors: The Journal of the Human Factors and Ergonomics Society*, vol. 57(1): 144–162, 2015.

M. Dagdelen, G. Reymond, A. Kemeny, M. Bordier and N. Maïzi, **MPC Based Motion Cueing Algorithm: Development and Application to the ULTIMATE Driving Simulator**, in Proceedings of the Driving Simulation Conference 2004 Europe, Paris, France, 221–233, 2004.

M. Dagdelen, G. Reymond, A. Kemeny, M. Bordier and N. Maïzi, **Model-based predictive motion cueing strategy for vehicle driving simulators**, *Control Engineering Practice*, vol. 17: 995–1003, 2009.

M. Diehl, H. Bock, J. P. Schlöder, R. Findeisen, Z. Nagy and F. Allgöwer, **Real-Time Optimization and Nonlinear Model Predictive Control of Processes Governed by Differential-Algebraic Equations**, *Journal of Process Control*, vol. 12: 577–585, 2002.

N. J. Garrett and M. C. Best, **Model predictive driving simulator motion cueing algorithm with actuator-based constraints**, *Vehicle System Dynamics*, vol. 51(8): 1151–1172, 2013.

P. R. Grant and L. D. Reid, **Motion Washout Filter Tuning: Rules and Requirements**, *Journal of Aircraft*, vol. 34(2): 145–151, 1997.

E. Groen and W. Bles, **How to use body tilt for the simulation of linear self motion**, *Journal of Vestibular Research: Equilibrium and Orientation*, vol. 14(5): 375–385, 2004.

M. Katliar, K. N. De Winkel, J. Venrooij, P. Pretto and H. H. Bülthoff, **Impact of MPC Prediction Horizon on Motion Cueing Fidelity**, in Proceedings of the Driving Simulation Conference 2015 Europe, Tübingen, Germany, 2015.

M. Katliar, J. Fisher, G. Frison, M. Diehl, H. Teufel and H. H. Bülthoff, **Nonlinear Model Predictive Control of a Cable-Robot-Based Motion Simulator.**, in International Federation of Automatic Control, 2017.

M. Katliar, F. Drop, H. Teufel, M. Diehl and H. H. Bülthoff, **Real-Time Nonlinear Model Predictive Control of a Motion Simulator Based on a 8-DOF Serial Robot.**, in 17th European Control Conference (ECC 2018), 2018.

T. D. van Leeuwen, D. Cleij, D. M. Pool, M. Mulder and H. H. Bülthoff, **Time-varying perceived motion mismatch due to motion scaling in curve driving simulation**, *Transportation Research Part F: Traffic Psychology and Behaviour*, vol. 61: 84–92, 2019.

J. R. van der Ploeg, **Sensitivity Analysis of a Model Predictive Control-based Motion Cueing Algorithm**, Master's thesis, Delft University of Technology, 2018, http://resolver.tudelft.nl/uuid:4ec1adda-1afd-4b7f-85f5-3b2a64db9dbe.

J. Venrooij, P. Pretto, M. Katliar, S. Nooij, A. Nesti, M. Lächele, K. N. de Winkel and D. Cleij, **Perception-based motion cueing: validation in driving simulation**, in Proceedings of the 2015 Driving Simulation Conference, Tübingen, Germany, 2015.